20

Estimation of the effective scattering properties during tissue cryodestruction performed by the sapphire cryoprobe

© I.N. Dolganova[1], A.K. Zotov[1], L.P. Safonova[2], K.I. Zaytsev[3], V.N. Kurlov[1]

[1] Osipyan Institute of Solid State Physics of RAS,
142432 Chernogolovka, Moscow Region, Russia
[2] Bauman Moscow State Technical University, 105005 Moscow, Russia
[3] Prokhorov Institute of General Physics, Russian Academy of Sciences, 119991 Moscow, Russia

e-mail: in.dolganova@gmail.com

Received January 24, 2023
Revised January 27, 2023
Accepted February 01, 2023.

The task of monitoring the condition of the tissue during its cryodestruction is extremely relevant for cryosurgery. Previously, the concept of a sapphire cryoprobe was proposed, which makes it possible to detect diffusely scattered light from a tissue during an ice ball formation. This probe combines the advantages of sapphire as a promising material for cryosurgery, as well as the possibility of assessing the depth of tissue freezing in the contact area. The use of several light source channels inside the applicator, spaced at different distances from the detector channel, makes it possible to analyze the scattering properties of the medium using the methods of diffusion theory. In this paper, we consider the influence of the position and number of analyzed source channels on the signals recorded by the detector channel and the determined effective scattering coefficient of a two-component medium consisting of an iceball and unfrozen tissue. Differences in the scattering coefficient obtained for various channel configurations are shown, as well as the advantages of analyzing a large number of channels to describe the effective properties of the medium with a complex iceball boundary.

Keywords: sapphire, cryosurgery, cryoprobe, diffuse scattering, scattering coefficient

DOI: 10.61011/EOS.2023.06.56660.121-23

Introduction

The use of low temperatures, which is the basis of cryosurgery, leads to the formation of ice crystals inside the tissue, that damage the tissue and cause hypoxia and apoptosis [1–4]. Due to this, cryosurgery is used to remove certain tissue areas, in particular, neoplasms of various nosologies and localizations[5,6], being a minimally invasive and relatively painless method compared to classical surgery methods [7]. To achieve the desired efficiency, the tissue temperature must fall below the threshold of cell death, which is in the range from -20 to -40°C, thus forming a so-called iceball. This is achieved through the use of special tools, known as cryoprobes, which may be of different implementations and principles of operation [6,8–11]. They provide the desired rate of cooling and freezing of the tissue through the use of materials with high thermal conductivity. Metal probes based on the Joule-Thomson and Peltier effects are widely used, along with the probes cooled by the use of various refrigerants, for example, liquid nitrogen.

An important task in the course of cryosurgical operation is monitoring of the tissue condition in the process of exposure to low temperatures because there is a risk of damage to surrounding healthy tissues, as well as a risk of formation of a smaller iceball and, as a consequence, insufficient impact on the tissue area of interest. Therefore, cryosurgical manipulations are often accompanied by additional monitoring methods, namely: ultrasonic diagnostics, magnetic resonance and computer-assisted tomography, thermometry [12–15]. Along with this, the promising potential of optical monitoring methods has been shown [16–18], in particular, the use of acoustooptic systems [16,17]. However, these methods do not allow solving the problem of combining the cryoprobe and monitoring functions in one compact instrument.

Previously, the authors have proposed a sapphire cryoprobe that implements optical monitoring of the tissue freezing process due to detection of diffuse reflected intensities of tissue optical response [19]. Sapphire has high thermal conductivity at low temperatures, high hardness, chemical inertness, resistance to low temperatures and aggressive environments, as well as optical transparency in a wide wavelength range, which makes it possible to deliver optical radiation to tissues through the end face of such a probe [20,21]. It has also been shown that sapphire probes make it possible to obtain a greater iceball volume and a higher tissue cooling rate compared to metal probes, all other things being equal [11]. In the proposed cryoprobe design the diffuse response of the medium is recorded during the operation of four source channels located at different distances from the detector channel. This makes it possible to restore the scattering properties of the medium, and also, by solving the inverse problem, to estimate the depth of tissue freezing [19].

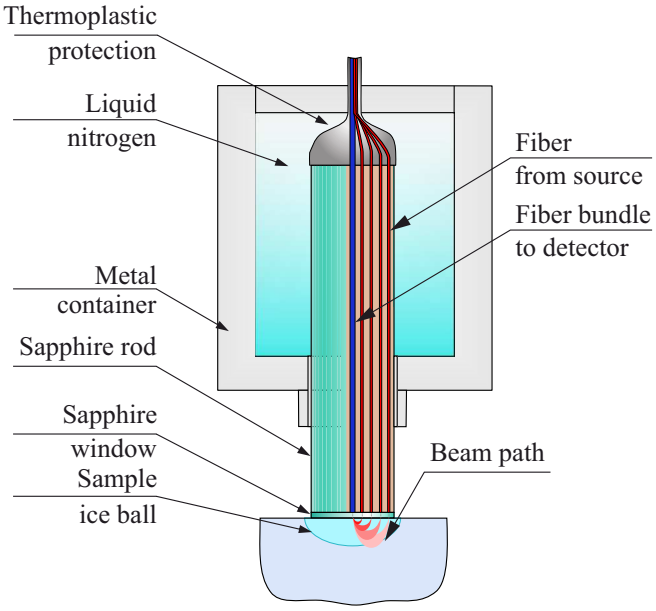

Figure 1. Scheme of the sapphire cryoprobe with the function of optical tissue monitoring in the process of cryodestruction.

In the proposed approach, all four channels of the radiation source are considered for the analysis and a plane-parallel model of the medium is used, where the upper layer corresponds to frozen tissue, and the lower, semi-infinite level corresponds to non-frozen tissue. However, in reality the interface between these layers has a complex shape, approaching a hemispherical shape in the process of ice ball growth, which distorts the scattered radiation intensities recorded by the detector. This study investigates the effect of position of the source channels on the recorded signals and the determined effective values of the scattering coefficient of a two-component medium. For the analysis, the experimental data obtained using a gelatin-based tissue phantom with the addition of intralipid are used.

Experimental technique

The sapphire cryoprobe is described in details in [19]. Fig. 1 shows schematically the probe in contact with the medium. The diameter of the sapphire rod, produced by the edge-defined film-fedgrowth (EFG) technique for growing profiled crystals [22–24], is 12.5 mm, its length is 125 mm. Cooling is achieved by immersing the upper part of the rod in liquid nitrogen. The rod has hollow channels inside containing optical fibers with a diameter of 200 μm, which are connected to the radiation source, and a fiber bundle with a diameter of 1.25 mm, which is connected to the detector. They are connected to a Oxiplex TS (ISS, USA) commercial system, which is used to record the intensity of diffusely scattered radiation when the medium is exposed to the impact of a frequency-modulated (110 MHz) source with a wavelength of 692 nm. The source fibers are fixed in a metal mandrel, which is placed in the appropriate channel of the rod. In the following text the term „source channels“ is used for simplicity, meaning the fibers connected to the radiation source. The fiber bundle connected to the detector, i.e. the „detector channel“, is located in the center of the sapphire rod. Distances between the source and detector channels are $R_1 = 2.11$, $R_2 = 3.34$, $R_3 = 4.57$, $R_4 = 6.42$ mm. The contact part of the probe is closed with a plane-parallel 0.9-mm-thick sapphire window to protect the end of the fibers and the fiber bundle from direct contact with the biological medium.

The optoelectronic part of the probe records alternating (AC), direct (DC) and phase (PH) components of the radiation intensity. This makes it possible to reconstruct the scattering and absorption coefficients of measured media. Deemed trajectories of recorded photons are also shown in Fig. 1. It can be seen that with a small iceball thickness, the trajectory intersects the ice front, and with an increase in the volume of the iceball, the intersection is preserved only for the channels located at the edge of the probe.

To restore the scattering coefficient of the medium in the presence of a frequency-modulated radiation source and spatially separated source channels and the detector channel, the method of analyzing the intensity of diffusely scattered radiation is used, which is described in a number of publications [25–29]. In the approximation of a semi-infinite medium, the dependences of the phase component $\mathrm{PH}(R)$ and the DC-component $\ln(R^2\mathrm{DC})$ of intensity on the distance between the source and detector channels are considered. These dependencies are approximated by straight lines with corresponding slopes S_{DC} and S_{PH}. The absorption coefficient μ_a and the reduced scattering coefficient μ_s' are determined from the following relationships:

$$\mu_a = -\frac{\omega}{2c}\frac{S_{\mathrm{DC}}}{S_{\mathrm{PH}}}\left(\frac{S_{\mathrm{DC}}^2}{S_{\mathrm{PH}}^2}+1\right)^{-\frac{1}{2}}, \tag{1}$$

$$\mu_s' = \frac{S_{\mathrm{DC}}^2}{3\mu_a} - \mu_a, \tag{2}$$

where ω is modulation frequency of the radiation source, c is speed of light in the medium. The reduced scattering coefficient is related to the anisotropy parameter g and the scattering coefficient of the medium by the following relationship: $\mu_s' = \mu_s(1-g)$.

Thus, using (1) and (2) and the values of the intensity of diffusely scattered radiation measured over a certain period of time, it is possible to obtain the time dependences of the effective absorption and scattering coefficients. When analyzing a medium during the formation of an iceball in it, the obtained values will characterize a two-component system composed of layers of frozen and non-frozen medium.

It is worth noting that typical values of the absorption coefficient in tissues are significantly less than the values of the reduced scattering coefficient [30]. Their changes in the process of tissue freezing are also not significant, therefore,

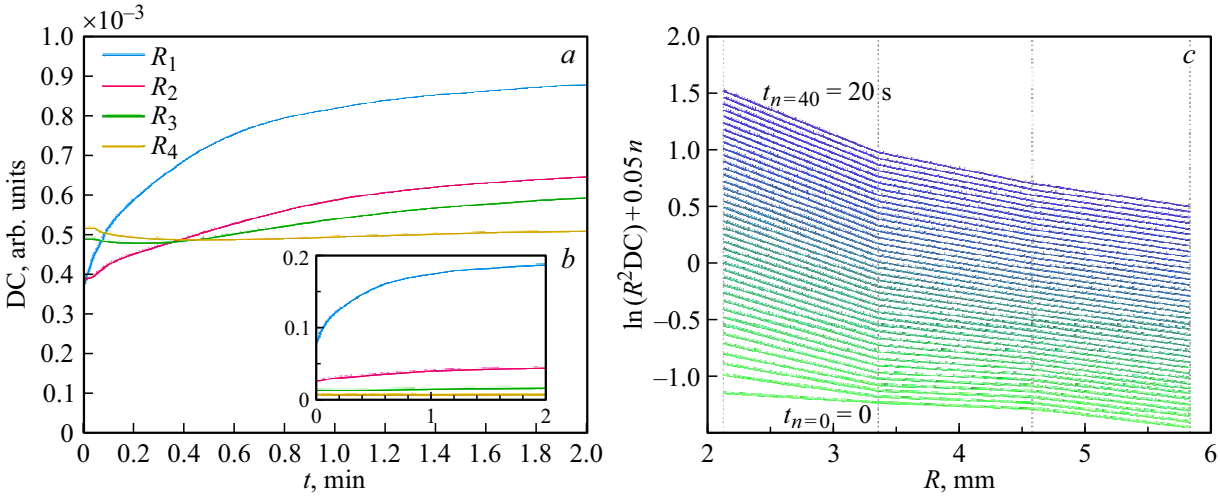

Figure 2. Results of measuring the intensity of diffusely scattered radiation using a sapphire cryoprobe in the process of formation of an iceball in a tissue phantom based on gelatin gel and intralipid. (a) Time dependence of the DC-component intensity obtained for different source channels located at $R_1 = 2.11$, $R_2 = 3.34$, $R_3 = 4.57$, $R_4 = 6.42$ mm away from the detector channel. (b) Time dependence of the DC-component intensity with corrections obtained after calibration of the cryoprobe. (c) Logarithmic dependence of $\ln(R^2\mathrm{DC})$ on distance R, shown for the first 20 s after probe contact with phantom (time sequence of 40 curves is shown).

they are not considered in this study. Nevertheless, the study of the absorption coefficient in the future may be of interest to obtain additional information about the condition of the tissue in the process of cryodestruction.

For experimental studies, a biological tissue phantom based on a water-based gelatin gel with the addition of 2% intralipid (20%, Fresenius Kabi, Germany) was chosen. The phantom was preheated to a temperature of 37°C to slow down the process of iceball formation. The phantom size significantly exceeded the diameter of contact area of the sapphire probe.

The optical part of the cryoprobe was calibrated using test objects with known scattering and absorption coefficients. Then the probe was cooled by filling its reservoir with liquid nitrogen (Fig. 1) and, after stabilization of its temperature, was brought into contact with the gelatin-based phantom. The radiation intensity was measured for 3 min. Results are presented in following section.

Results

Fig. 2, a shows values of the DC-component of the radiation intensity. It can be seen that the nearest two channels are characterized by an increase in intensity followed by saturation. At the same time, a decrease in intensity followed by an increase in it can be noted for the 3rd and the 4th channels at some point in time. Probably, this effect is due to the uneven surface of the iceball on its periphery and a smoother shape in the central part at the initial moment of the frozen area formation. After introducing the corrections obtained by calibrating the probe against a known test object (Fig. 2, b), the described intensity dynamics in these channels becomes almost unnoticeable.

Fig. 2, c shows the logarithmic dependence of $\ln(R^2\mathrm{DC})$ on the channel position after the calibration against a known test object. For homogeneous media, this dependence should have the form of a straight line; however, in the considered case, the behavior of the presented dependences is different. It is clear that the presence of two layers with a curvilinear interface between them has a different effect on the intensity of diffusely scattered radiation measured for each channel. For the following analysis of the effective scattering parameters of such an object, sections of the $\ln(R^2\mathrm{DC})$ dependencies were considered separately for channels 1-2, 2-3, 3-4, 1-2-3, 2-3-4, 1-2-3-4. In each case, the corresponding approximating values of the slope S_{DC} were found and relationships (1) and (2) were used to assess the dynamics of the effective properties of the medium.

Results of calculating the effective reduced scattering coefficient for the selected combinations of channels are shown in Fig. 3. It can be seen that taking into account the first channel results in a noticeable increase in μ_s'. This is due to the greater thickness of the iceball in the central part compared to the peripheral areas. Another possible cause is the increase in the intensity of the radiation reflected from the window-sample interface due to a change in the refractive index of the medium after freezing. Taking into account the aperture of the fibers used, the contribution of this component is significantly reduced for far channels. Taking into account the fourth channel results in a smooth growth of the scattering coefficient curve because it is characterized by a larger probing depth in the medium compared to other channels and a smaller iceball thickness, i.e. the tissue freezing front stays within the probing depth

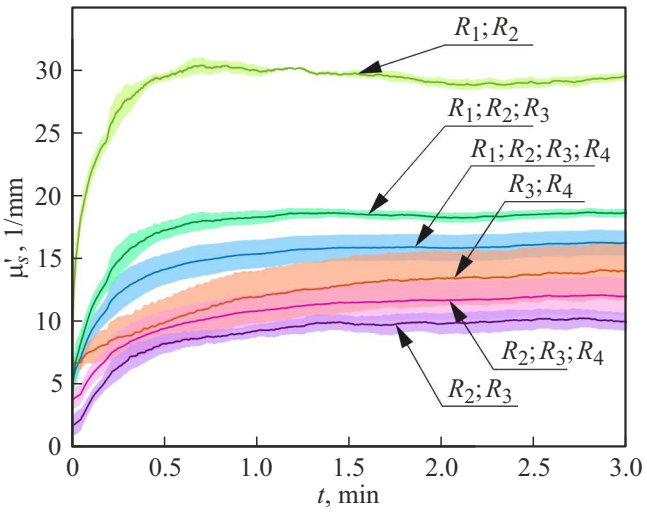

Figure 3. Dynamics of the change in the effective reduced scattering coefficient μ_s', obtained for various combinations of source channels located at R_i away from the detector channel. The error region corresponds to the $\pm\sigma$ values.

for a longer time. The analysis of combinations of channels 3-4 and 2-3-4 shows that the obtained data for μ_s' are within the measurement accuracy, however, a larger number of channels makes it possible to more accurately evaluate the effective values of the medium properties. It should also be noted that the real interface between the layers of the medium is not planar, the reflection of the radiation fraction from it can be the cause of that the response of the medium is attenuated more strongly for peripheral channels (i.e., $\mu_s'(R_3, R_4) > \mu_s'(R_2, R_3)$), where this interface has a significant slope with respect to the plane of the contact area of the probe.

The obtained results confirm that the choice of a channels combination 1-2-3-4 is preferable for evaluating the effective scattering properties of the entire sample in the area of cryoprobing, however, the previously adopted plane-parallel model of the medium used to further restore the iceball depth requires clarification. At the same time, pairwise consideration of neighboring channels leads to significant differences in the scattering coefficient, so their analysis can be used to describe the shape of the iceball, supplementing the algorithm proposed earlier in [19].

It is clear that the obtained values of the effective scattering coefficient are affected by a number of factors, some of which have already been noted in this text:

−reflection from the interface between the protective window and the sample;

−shape of the interface between frozen and non-frozen medium;

−information about the refractive index of the medium in two states;

−evenness of distribution of optical properties over the volume of the medium.

These factors determine the direction for further research of the developed tool and method for monitoring the medium in the process of cryoprobing. Analysis of their effect assumes a series of experimental studies and numerical modeling.

Conclusion

The operation of a sapphire probe for cryosurgery is considered, namely, the function of determining the effective scattering properties of the medium. The probe, which has four source channels at different distances from the detector channel, makes it possible to record the diffusely scattered response of the medium in the process of iceball formation in it. The effective values of the reduced scattering coefficient of a two-component medium consisting of a layer of frozen tissue and a layer of non-frozen tissue are calculated from the obtained signals using the diffusion theory. It is shown that the time-varying curvilinear iceball interface affects the intensity of diffusely scattered radiation measured for each channel. The use of a larger number of channels allows the most efficient determination of the average scattering properties of the medium. Nevertheless, the scattering coefficient analysis performed for pairs of adjacent channels can be further used to describe the iceball shape.

Conflict of interest

The authors declare that they have no conflict of interest.

References

[1] J.G. Baust, A.A. Gage. BJU International, **95** (9), 1187 (2005). DOI: 10.1111/j.1464-410X.2005.05502.x

[2] A.A. Gage, J.M. Baust. Cryobiology, **37** (3), 171 (1998). DOI: 10.1006/cryo.1998.2115

[3] A.A. Gage, J.M. Baust, J.G. Baust. *Cryobiology*, **59** (3), 229 (2009). DOI: 10.1016/j.cryobiol.2009.10.001

[4] N.N. Korpan. *Basics of Cryosurgery* (Springer, Vienna, 2001). DOI: 10.1007/978-3-7091-6225-5

[5] D.A. Kunkle, R.G. Uzzo. Cancer, **113** (10), 2671 (2008). DOI: 10.1002/cncr.23896

[6] B. Surtees, S. Young, Y. Hu, G. Wang, E. McChesney, G. Kuroki, P. Acree, S. Thomas, T. Blair, S. Rastogi, D.L. Kraitchman, C. Weiss, S. Sukumar, S.C. Harvey, N.J. Durr. PLOS ONE, **14** (7), 1 (2019). DOI: 10.1371/journal.pone.0207107

[7] E. Vansonnenberg, W. McMullen, L. Solbiati, T. Livraghi, P. Müeller, S. Silverman. *Tumor Ablation: Principles and Practice* (Springer-Verlag, New York, 2005). DOI: 10.1007/0-387-28674-8

[8] R.C. Ward, A.P. Lourenco, M.B. Mainiero. Am. J. Roentgen., **213** (3), 716 (2019). DOI: 10.2214/AJR.19.21329

[9] A. Dhaliwal, S. Saghir, H. Mashiana, A. Braseth, B. Dhindsa, D. Ramai, P. Taunk, R. Gomez-Esquivel, A. Dam, J. Klapman, D. Adler. World J. Gastrointest. Endosc., **14** (1), 17 (2022). DOI: 10.4253/wjge.v14.i1.17

[10] I.A. Burkov, A.V. Pushkarev, S.S. Ryabikin, A.V. Shakurov, D.I. Tsiganov, A.A. Zherdev. Int. J. Refriger., **133**, 30 (2022). DOI: 10.1016/j.ijrefrig.2021.10.020
[11] A.V. Pushkarev, S.S. Ryabikin, D.I. Tsiganov, A.K. Zotov, V.N. Kurlov, I.N. Dolganova. J. Biomed. Photon. Engin., **8** (4), 040501 (2022). DOI: 10.18287/JBPE22.08.040501
[12] M. Ahmed, J. Weinstein, J. Hussain, A. Sarwar, M. Anderson, B. Dillon. CardioVascular and Interventional Radiology, **41**, 298 (2018). DOI: 10.1007/s00270-017-1801-3
[13] J. Tokuda, L. Chauvin, B. Ninni, T. Kato, F. King, K. Tuncali, N. Hata. Phys. Med. Biol., **63** (8), 085010 (2018). DOI: 10.1088/1361-6560/aab736
[14] J. Pohlan, W. Kress, K.-G. Hermann, J. Mews, M. Kroes, B. Hamm, T. Diekhoff. J. Comp. Assist. Tomogr., **44** (5), 744 (2020). DOI: 10.1097/RCT.0000000000001081
[15] Y. Yang, Y. Li, Y. Wu, S. Qiu, C. Liu, Q. Wang, Y. Hong, J. Lyu, Y. Zhang, D. Du. Cryobiology, **92**, 203 (2020). DOI: 10.1016/j.cryobiol.2020.01.012
[16] K. Larin, I. Larina, M. Motamedi, R. Esenaliev. Quant. Electron., **32** (11), 953 (2002). DOI: 10.1070/QE2002v032n11ABEH002327
[17] R.O. Esenaliev. J. Biomed. Opt., **22** (9), 091512 (2017). DOI: 10.1117/1.JBO.22.9.091512
[18] A.K. Zotov, A.A. Gavdush, G.M. Katyba, L.P. Safonova, N.V. Chernomyrdin, I.N. Dolganova. J. Biomed. Opt., **26** (4), 043003 (2021). DOI: 10.1117/1.JBO.26.4.043003
[19] I.N. Dolganova, A.K. Zotov, L.P. Safonova, P.V. Aleksandrova, I.V. Reshetov, K.I. Zaytsev, V.V. Tuchin, V.N. Kurlov. J. Biophotonics, **16** (3), e202200288 (2022). DOI: 10.1002/jbio.202200288
[20] G. Katyba, K. Zaytsev, I. Dolganova, I. Shikunova, N. Chernomyrdin, S. Yurchenko, G. Komandin, I. Reshetov, V. Nesvizhevsky, V. Kurlov. Progr. Cryst. Gr. Charact. Mater., **64** (4), 133 (2018). DOI: 10.1016/j.pcrysgrow.2018.10.002
[21] *Encyclopedia of Materials: Science and Technology*, ed. by K.J. Buschow, R.W. Cahn, M.C. Flemings, B. Ilschner, E.J. Kramer, S. Mahajan, P. Veyssiére (Elsevier, Oxford, 2001), P. 8259–8264. DOI: 10.1016/B0-08-043152-6/01478-9
[22] H. LaBelle, J. Cryst. Growth, **50** (1), 8 (1980). DOI: 10.1016/0022-0248(80)90226-2
[23] V. Kurlov, S. Rossolenko. J. Cryst. Growth, **173** (3), 417 (1997). DOI: 10.1016/S0022-0248(96)00836-6
[24] P.I. Antonov, V.N. Kurlov. Crystallogr. Rep., **47** (1), S43 (2002). DOI: 10.1134/1.1529958
[25] M.A. Franceschini, S. Fantini, L.A. Paunescu, J.S. Maier, E. Gratton. Appl. Opt., **37** (31), 7447 (1998). DOI: 10.1364/AO.37.007447
[26] S. Fantini, M.A. Franceschini, J.B. Fishkin, B. Barbieri, E. Gratton. Appl. Opt., **33** (22), 5204 (1994). DOI: 10.1364/AO.33.005204
[27] S. Fantini, M.A. Franceschini, E. Gratton. J. Opt. Soc. Am. B, **11** (10), 2128 (1994). DOI: 10.1364/JOSAB.11.002128
[28] B.W. Pogue, M.S. Patterson. Phys. Med. Biol., **39** (7), 1157 (1994). DOI: 10.1088/0031-9155/39/7/008
[29] A. Liemert, A. Kienle. Opt. Express, **18** (9), 9456 (2010). DOI: 10.1364/OE.18.009456
[30] A. Bashkatov, E. Genina, V. Tuchin, in *Handbook of Biomedical Optics*, ed. by D.A. Boas, C. Pitris, N. Ramanujam, (CRC Press, Boca Raton, 2011), P. 67.

Translated by Y.Alekseev